Acta Crystallographica Section C
Crystal Structure Communications
ISSN 0108-2701

α-Tris(2,4-pentanedionato-κ^2O,O')-chromium(III) at 290 and 110 K: a new δ phase at 110 K

Lars S. von Chrzanowski, Martin Lutz* and Anthony L. Spek

Bijvoet Center for Biomolecular Research, Crystal and Structural Chemistry, Utrecht University, Padualaan 8, 3584 CH Utrecht, The Netherlands
Correspondence e-mail: m.lutz@chem.uu.nl

Received 27 June 2007
Accepted 10 July 2007
Online 26 July 2007

The crystal structure of the title compound, $[Cr(C_5H_7O_2)_3]$, has been determined at 290 and 110 K to provide information on thermal vibrations and disorder. The α polymorph at room temperature has been reported [Morosin (1965). *Acta Cryst.* **19**, 131–137]. The reinvestigation of this structure, presented here, indicates the presence of weak uninterpretable supercell reflections together with disorder streaks. The discussed structure can thus be considered as an average structure. After cooling to 110 K, a new δ polymorph was found, which is a superstructure of the α polymorph. The space group remains $P2_1/c$ and the phase transition can therefore be considered as *klassengleich*. The unit-cell volume increases by a factor of six, resulting in six independent molecules in the asymmetric unit.

Comment

Metal atoms, especially transition metals, are present in the active centers of almost one-third of all known enzymes and play an important role in catalytic processes. Cr^{III} is an essential trace element (Goldhaber, 2003) with the important function of maintaining the normal glucose metabolism in the human body, in particular at advanced age or in the case of diabetes. Trivalent metal acetylacetonate complexes [M^{III}(acac)$_3$; acac is acetylacetonate or 2,4-pentanedionate] belong to the β-diketonates and are a particularly accessible species for studying structure, bonding and ligand coordination in organometallic systems. Owing to their high volatility, β-diketonates of metals are used as precursors in the process of chemical deposition of coatings from the vaporous phase, which is known to be a promising technique for the production of, for example, superconducting materials and nano-sized coatings (Naumov *et al.*, 2006).

It is well known that these complexes show polymorphism; an overview is given by Sabolović *et al.* (2004). Phase transitions of these compounds are observed at low temperatures; for Mn(acac)$_3$, see Geremia & Demitri (2005), and for Al(acac)$_3$, see von Chrzanowski *et al.* (2007*a*). M^{III}(acac)$_3$ can be grouped into a polymorphous series of three. By an old nomenclature of Astbury & Morgan (1926), the α polymorph crystallizes in the monoclinic crystal system with the space group $P2_1/c$. To our knowledge, all previous studies of Cr(acac)$_3$, (I), have been carried out at room temperature, with the compound crystallizing as its α polymorph (*e.g.* Morosin, 1965). In the known studies of the α polymorphs, the C atoms show anomalous displacement parameters and disorder, especially in one of the three ligands (*e.g.* Hon & Pfluger, 1973). In the course of our ongoing studies of trivalent metal acetylacetonates and in order to investigate this behavior, we report here the redetermination of α-Cr(acac)$_3$ at 290 K, (I*a*), and a new determination at 110 K, (I*b*). At 110 K, we observed a new δ phase.

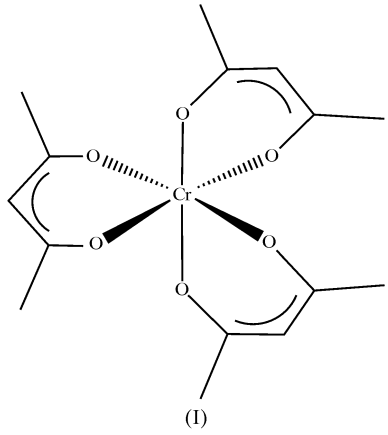

(I)

As mentioned previously, M^{III}(acac)$_3$ complexes show anomalous displacement parameters and disorder, especially in one of the three acac ligands, labeled C11–C15. We reported this observation in our previous temperature-dependent studies of α-Al(acac)$_3$ (von Chrzanowski *et al.*, 2007*a*) and α-Co(acac)$_3$ (von Chrzanowski *et al.*, 2007*b*). This can also be seen in the room-temperature structure of (I) reported by Morosin (1965), (I*m*), as well as in the present study of (I*a*) at 290 K (Figs. 1*a* and 1*b*). Rigid-body analyses for both structures (Schomaker & Trueblood, 1998) result in relatively high agreement factors of $R = 0.204$ for (I*m*) and $R = 0.131$ for (I*a*) [$R = \{\sum[w(U_{obs} - U_{calc})]^2/\sum(wU_{obs})^2\}^{1/2}$]. As a result of different weighting, the agreement factor for (I*m*) is significantly higher; for (I*a*), the weights were derived from the standard uncertainties of the anisotropic displacement parameters, while for (I*m*), unit weights were used because no standard uncertainties are given in the paper. Difference plots (Hummel *et al.*, 1990) between the observed displacement parameters and the rigid-body models indicate large internal motions (Figs. 1*c* and 1*d*).

This anomalous behavior is also manifested in the CCD detector images of (I*a*) by the presence of diffuse disorder streaks between the reflections (Fig. 2), on which some intensity maxima are present. These maxima were not interpreted because of their weakness. The presence of large isolated diffuse spots/areas was also reported in (I*m*) and there explained by thermal motion. On the basis of our data, we assume that (I*a*) actually has a larger unit cell, which

 DOI: 10.1107/S0108270107033823

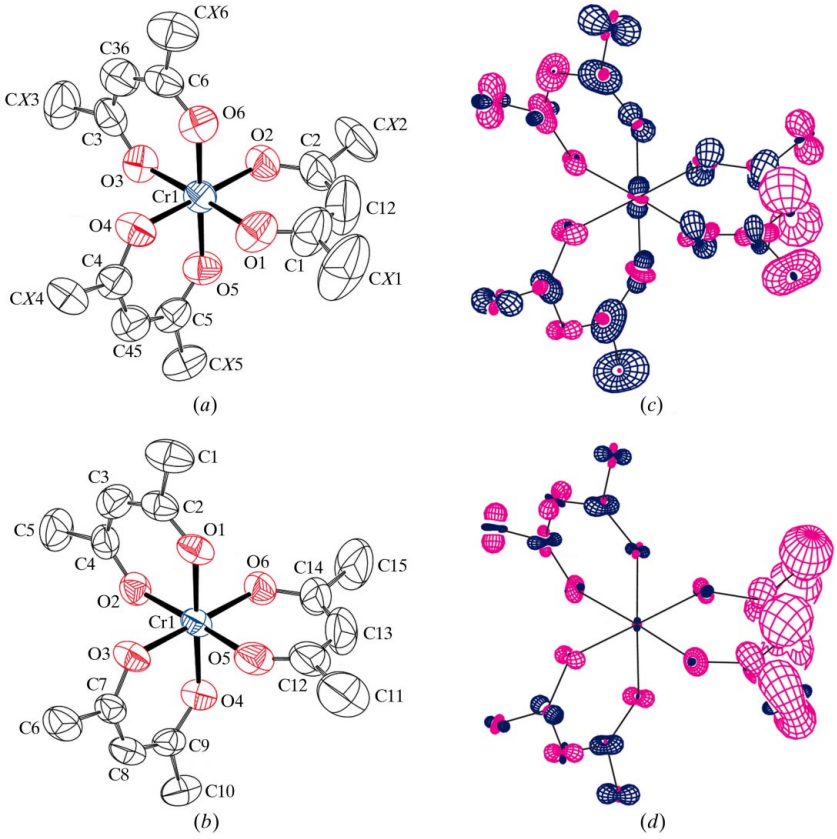

Figure 1
Left: displacement ellipsoid plots and atomic numbering schemes of (I), showing (*a*) the literature structure of (I*m*) (Morosin, 1965) at room temperature with the original atomic numbering scheme and (*b*) (I*a*) at 290 K. Ellipsoids are drawn at the 50% probability level and H atoms have been omitted for clarity. Right: peanut plots (Hummel *et al.*, 1990) showing the difference between the measured displacement parameters and the parameters obtained by rigid-body analyses using the program *THMA11* (Schomaker & Trueblood, 1998). A scale factor of 3.08 was used for the r.m.s. surfaces. [In the electronic version of the paper, blue spheres (darker here) indicate positive differences and purple spheres (lighter here) negative differences.] (*c*) The literature structure of Morosin (1965) at room temperature and (*d*) (I*a*) at 290 K. The plots are drawn in the same orientation as the displacement ellipsoid plots and have the same atomic numbering schemes.

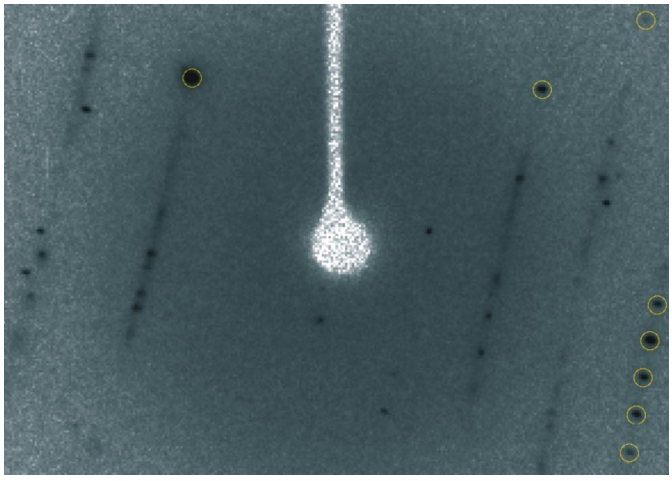

Figure 2
A CCD detector image of (I*a*) at 290 K, showing diffuse disorder streaks between reflections. Predicted reflections of the 1706.01 (18) Å^3 unit cell are circled.

corresponds to the low-temperature δ polymorph (see below), and by ignoring the weak supercell reflections an average structure was obtained.

At 110 K, the diffraction pattern shows supercell reflections, which are now interpretable, and the structure of a new δ polymorph (I*b*) could be determined. Because this supercell is probably already present in (I*a*), an exact temperature range for the phase transition cannot be determined. The transformation matrix from the high-temperature α polymorph to the new low-temperature δ polymorph is (200/010/003). The determinant of this matrix is six and therefore the cell volume increases by a factor of six. Interestingly, the application of this transformation matrix to the coordinates of (I*a*) at the chosen origin to generate the coordinates of (I*b*) leads to a false minimum. Solution attempts of (I*b*) from scratch with the programs *SIR97* (Altomare *et al.*, 1999), *SIR2000* (Burla *et al.*, 2000) or *DIRDIF99* (Beurskens *et al.*, 1999) using standard parameters led to the same false minimum. In the false minimum, the structure can be refined to acceptable agreement factors, but the displacement parameters are unexpectedly large. The correct minimum was found by structure solution with the program *SHELXS97* (Sheldrick, 1997) using direct methods and corresponds to an origin shift of $\frac{1}{4}$ in the direction of the crystallographic *a* axis (Fig. 3). Refinement with the correct origin results in significantly improved agreement factors and, more importantly, completely normal

displacement parameters. With respect to the symmetry elements, the origin shift of $\frac{1}{4}$ means that exact inversion centers and 2_1 screw axes in (I*a*) become pseudosymmetry elements in (I*b*). In (I*b*), the space group remains $P2_1/c$, and the phase transition can thus be classified as *klassengleich*. A similar phase transition was observed in α-Al(acac)$_3$ (von Chrzanowski *et al.*, 2007*a*). There, the phase transition occurs between 150 and 110 K, and the transformation matrix from the high-temperature α polymorph to the low-temperature δ polymorph is $(10\bar{1}/0\bar{1}0/\bar{2}0\bar{1})$; the determinant of the matrix is three and the volume consequently increases by a factor of three.

The asymmetric unit of (I*b*) at 110 K consists of six independent molecules (Fig. 4). All molecules have approximately noncrystallographic D_3 symmetry, with r.m.s. deviations from ideal symmetry of between 0.128 Å for molecule 4 and 0.199 Å for molecule 5 (Pilati & Forni, 1998). All six molecules have essentially the same geometry, as can be seen in a quaternion fit (Fig. 5*a*). This quaternion fit (Mackay, 1984) considers only the molecular structures but does not take the crystal packing into account. The packing effects can be seen by the application of the transformation matrix to the α polymorph on the atomic coordinates of the δ polymorph. The result of this operation can be seen in Fig. 5(*b*). Two of the acac ligands have only small deviations after this averaging, while the third ligand (C11*X*–C15*X*) is severely affected by the packing. The latter ligand corresponds to the ligand with large displacement parameters (C11–C15) in the α polymorph, and therefore the phase transition can be considered as a disorder–order phase transition.

A possible explanation for this behavior is the presence of different C—H···O interactions (Table 3). Every ligand is a donor of one intermolecular C—H···O interaction with a range of C—H···O angles between 163 and 179°. The average C···O distance for the C11*X*–C15*X* ligand (*X* = 1–6 for molecules 1–6) is 3.57 (2) Å (for C15*X*—H···O4*Y*); this is the longest contact and therefore the weakest C—H···O interaction, resulting in the largest deviation for C11*X*–C15*X* (Table 4). The ligands appear to be split into two different groups; molecules 1, 2 and 4 define group 1, and molecules 3, 5 and 6 define group 2 (Table 5).

The ADDSYM routine of the program *PLATON* (Spek, 2003) indicates pseudo-translational symmetry for (I*b*) at 110 K. Such a situation has also been observed in the δ phase of Al(acac)$_3$ (von Chrzanowski *et al.*, 2007*a*), where two groups of reflections were present, *viz.* strong subcell reflections and weak supercell reflections. In (I*b*), three groups of reflections are present, *viz.* strong subcell reflections, and weak and very weak supercell reflections (Table 6). Nevertheless the weak supercell reflections are clearly present and prevent a transformation to the subcell.

A pseudo-translational symmetry test (*SIR97*; Altomare *et al.*, 1999) results in a value of 74% for the mean fractional scattering power of the electron density for reflections with $h = 2n$ and $l = 3n$ ($\langle E^2 \rangle = 4.734$), which is based on normalized structure factors from measured data (Cascarano *et al.*, 1985). The three highest vectors of nonzero length in the Patterson map, as calculated with *SHELXS97* (Sheldrick, 1997), end at (0.4994, 0.0000, 0.3332), (0.9996, 0.0000, 0.3332) and ($\frac{1}{2}$,0,0), again confirming the pseudo-translational symmetry of $\frac{1}{2}$ in the *a* and $\frac{1}{3}$ in the *c* direction.

Despite the pseudo-translational symmetry, a full matrix least-squares refinement with *SHELXL97* (Sheldrick, 1997) can be performed with default refinement parameters and without restraints or constraints. No correlation matrix elements were larger than 0.5. The weighting scheme for the refinement was optimized by *SHELXL97* based on all 18 651 unique reflections and results in a goodness-of-fit of 1.064. The corresponding goodness-of-fit for the 3155 strong subcell reflections without rerefinement and with the same weighting scheme is 1.748, and those for the 6296 weak and 9320 very weak supercell reflections are 1.038 and 1.029, respectively. Obviously the weighted σ values of the subcell reflections are underestimated.

A distribution diagram of all Cr—O bond distances shows a single maximum, and therefore the averaging of these distances is valid. A normal probability plot (Abrahams & Keve, 1971) of the low-temperature δ polymorph, in which all bond distances of each molecule are treated independently, results in a slope of 1.965. The observed outliers belong to the Cr—O distances. The range of Cr—O distances is wide; they range from 1.9460 (16) to 1.9750 (17) Å (Table 2). There is no

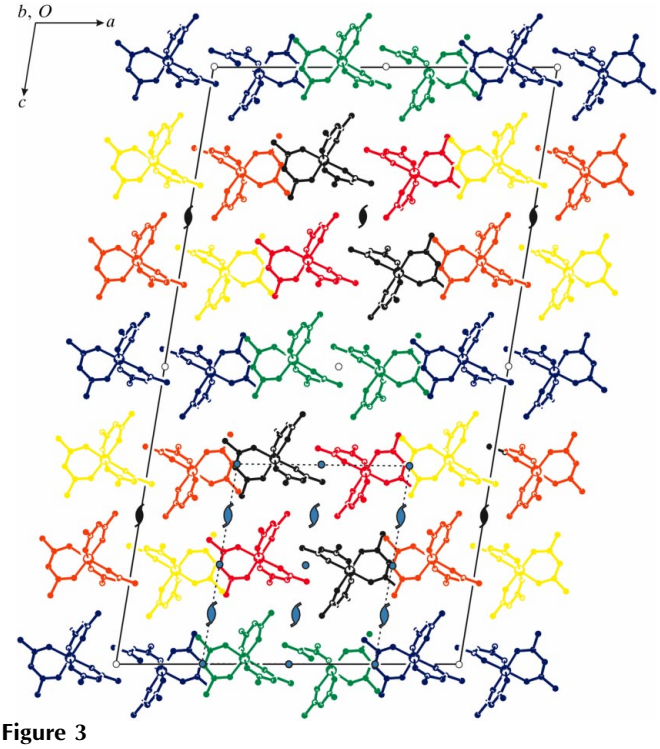

Figure 3
The crystal packing of (I*b*) at 110 K, viewed along the crystallographic *b* axis. The twofold screw axes are shown with black symbols and inversion centers are shown with unshaded circles. The unit cell of the high-temperature α phase is drawn with dashed lines; symbols for the screw axes and the inversion centers are shown shaded. Molecules of (I*a*) are not displayed. [In the electronic version of the paper, for the molecules of (I*b*), orange represents molecule 1 (*X* = 1), yellow molecule 2 (*X* = 2), blue molecule 3 (*X* = 3), green molecule 4 (*X* = 4), red molecule 5 (*X* = 5) and black molecule 6 (*X* = 6).]

chemical evidence for this large variance. This effect can be attributed to the internal motion of the molecules and the high standard uncertainties of the Cr—O bond distances. γ-Al(acac)$_3$ (von Chrzanowski *et al.*, 2006) and δ-Al(acac)$_3$ (von Chrzanowski *et al.*, 2007*a*) show similar variations of the corresponding Al—O bond distances, which range from 1.8790 (12) to 1.8909 (13) Å for γ-Al(acac)$_3$ and from 1.8704 (9) to 1.8910 (10) Å for δ-Al(acac)$_3$. The average values of Cr—O distances of the six independent molecules can be grouped into long Cr—O distances for molecules 2, 3 and 4 [1.9683 (Cr*X*—O4*X*) to 1.9673 Å (Cr*X*—O2*X*)] and short distances for molecules 1, 5 and 6 [1.9536 (Cr*X*—O6*X*) to

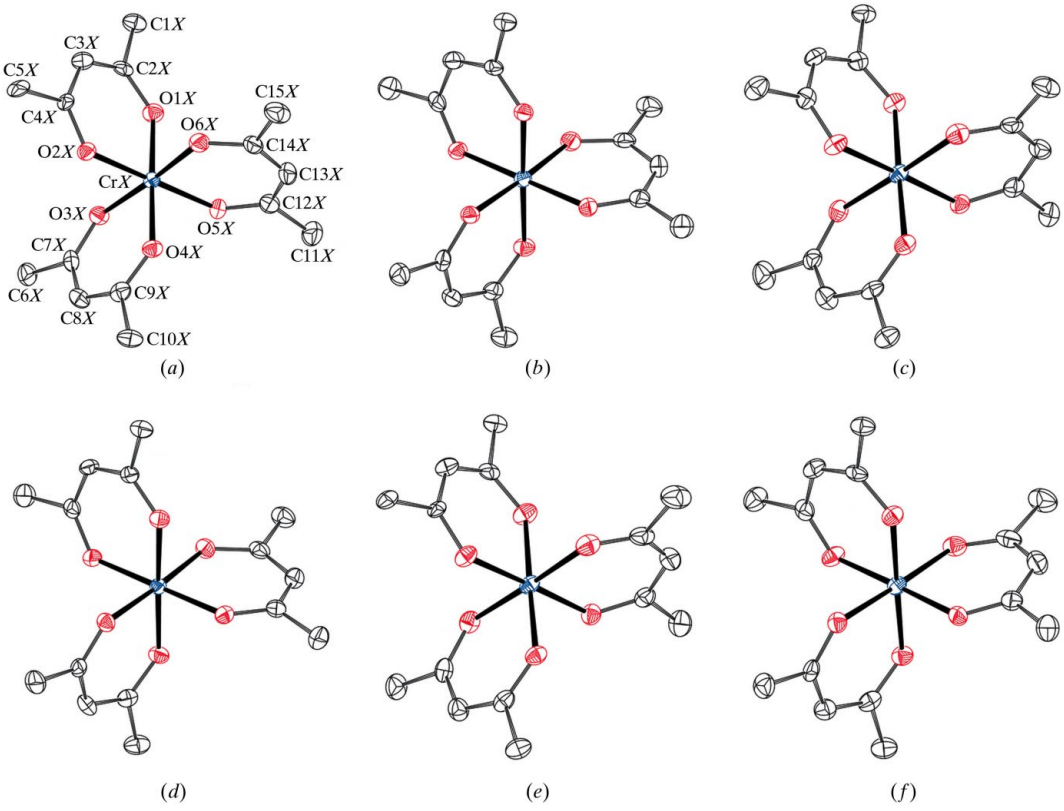

Figure 4
Displacement ellipsoid plots and atomic numbering schemes of the six independent molecules of (I*b*) at 110 K. All molecules are shown independently using the same orientation with the same atomic numbering scheme and do not represent the crystal packing. Ellipsoids are drawn at the 50% probability level. H atoms have been omitted for clarity. The views show (*a*) molecule 1 (*X* = 1), (*b*) molecule 2 (*X* = 2), (*c*) molecule 3 (*X* = 3), (*d*) molecule 4 (*X* = 4), (*e*) molecule 5 (*X* = 5) and (*f*) molecule 6 (*X* = 6).

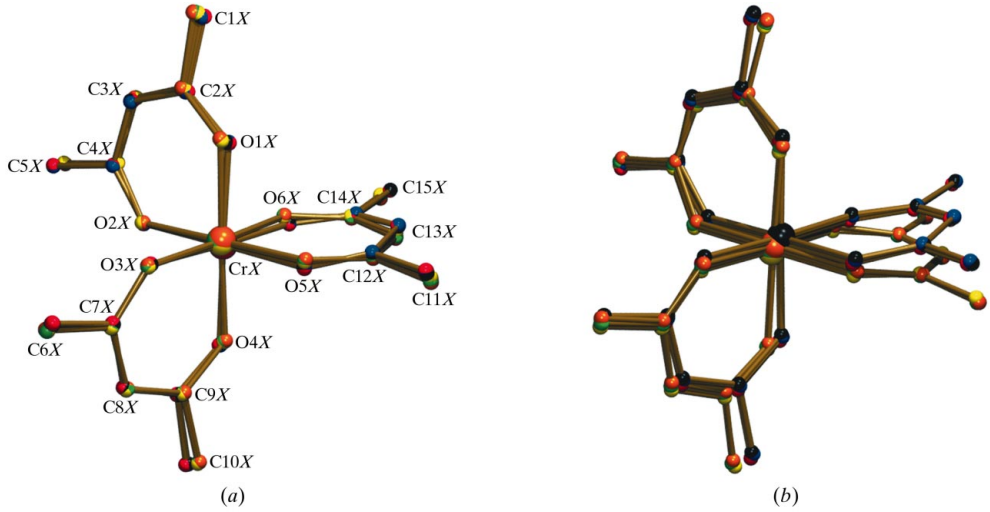

Figure 5
(*a*) Quaternion fit (Mackay, 1984) of the six independent molecules of (I*b*) at 110 K. (*b*) Transformation of the six independent molecules of (I*b*) at 110 K into an average structure using the transformation matrix between the α and δ polymorphs. (The color scheme for the electronic version is the same as in Fig. 3.)

1.9589 Å (CrX—O1X)]. Each long averaged Cr—O distance corresponds to a short distance on the opposite side.

This variation is also present in the high-temperature α polymorph (Ia), with Cr—O bond distances ranging between 1.9413 (18) and 1.9645 (17) Å (Table 1). The corresponding M—O distances in α-Al(acac)$_3$ and α-Co(acac)$_3$ show a similar variation (von Chrzanowski *et al.*, 2007*a*,*b*). Because octahedral Cr^{III} with electron configuration d^3 does not exhibit Jahn–Teller distortions (Wiberg, 1985), this variation can again only be explained by internal thermal motion. The thermal motion also contributes to a shortening of the Cr—O distances of the crystal structure determinations compared with 1.9773 Å obtained for Cr(acac)$_3$ from high-level density functional theory (DFT) (B3LYP/6–31G* for C, H, O and triple-ζ for Cr) calculations (Diaz-Acosta *et al.*, 2001).

Experimental

Violet crystals were obtained by slow evaporation of a solution of the commercially available material (Aldrich) in ethyl acetate at room temperature.

Determination (I*a*)

Crystal data

[Cr(C$_5$H$_7$O$_2$)$_3$]
M_r = 349.32
Monoclinic, $P2_1/c$
a = 13.9970 (8) Å
b = 7.5441 (4) Å
c = 16.3590 (12) Å
β = 99.031 (2)°
V = 1706.01 (18) Å^3
Z = 4
Mo $K\alpha$ radiation
μ = 0.69 mm^{-1}
T = 290 (2) K
0.30 × 0.27 × 0.12 mm

Data collection

Nonius KappaCCD diffractometer
Absorption correction: multi-scan (*SADABS*; Sheldrick, 2002)
T_{min} = 0.68, T_{max} = 0.92
45735 measured reflections
3924 independent reflections
3135 reflections with $I > 2\sigma(I)$
R_{int} = 0.030

Refinement

$R[F^2 > 2\sigma(F^2)]$ = 0.042
$wR(F^2)$ = 0.127
S = 1.04
3924 reflections
205 parameters
H-atom parameters constrained
$\Delta\rho_{max}$ = 0.34 e Å^{-3}
$\Delta\rho_{min}$ = −0.39 e Å^{-3}

Table 1
Selected bond lengths (Å) for (I*a*).

Cr1—O5	1.9413 (18)	Cr1—O3	1.9609 (16)
Cr1—O6	1.9548 (17)	Cr1—O2	1.9616 (16)
Cr1—O4	1.9572 (16)	Cr1—O1	1.9645 (17)

Determination (I*b*)

Crystal data

[Cr(C$_5$H$_7$O$_2$)$_3$]
M_r = 349.32
Monoclinic, $P2_1/c$
a = 27.5823 (2) Å
b = 7.4656 (1) Å
c = 48.6012 (4) Å
β = 99.2731 (3)°
V = 9877.09 (17) Å^3
Z = 24
Mo $K\alpha$ radiation
μ = 0.72 mm^{-1}
T = 110 (2) K
0.39 × 0.29 × 0.09 mm

Data collection

Nonius KappaCCD diffractometer
Absorption correction: multi-scan (*SORTAV*; Blessing, 1987)
T_{min} = 0.82, T_{max} = 0.94
101596 measured reflections
18651 independent reflections
9662 reflections with $I > 2\sigma(I)$
R_{int} = 0.052

Refinement

$R[F^2 > 2\sigma(F^2)]$ = 0.040
$wR(F^2)$ = 0.139
S = 1.06
18651 reflections
1225 parameters
H-atom parameters constrained
$\Delta\rho_{max}$ = 0.35 e Å^{-3}
$\Delta\rho_{min}$ = −0.60 e Å^{-3}

Table 3
Hydrogen-bond geometry (Å, °) for (I*b*).

D—H···A	D—H	H···A	D···A	D—H···A
C51—H51C···O52	0.98	2.49	3.465 (3)	172
C52—H52B···O53	0.98	2.45	3.423 (3)	173
C53—H53C···O51^{i}	0.98	2.52	3.470 (3)	163
C54—H54B···O55	0.98	2.46	3.438 (3)	173
C55—H55C···O56	0.98	2.49	3.458 (3)	169
C56—H56B···O54^{ii}	0.98	2.52	3.468 (3)	163
C101—H10C···O11^{iii}	0.98	2.60	3.584 (3)	179
C102—H10D···O12^{iv}	0.98	2.60	3.582 (3)	177
C103—H10I···O13^{iii}	0.98	2.53	3.509 (3)	176
C104—H10J···O14^{iv}	0.98	2.61	3.591 (3)	178
C105—H10O···O15^{iii}	0.98	2.56	3.533 (3)	173
C106—H10P···O16^{iv}	0.98	2.52	3.493 (3)	175
C151—H15B···O46^{iii}	0.98	2.61	3.580 (3)	172
C152—H15E···O45	0.98	2.61	3.587 (3)	172
C153—H15I···O44^{iii}	0.98	2.59	3.550 (3)	165
C154—H15K···O43^{iv}	0.98	2.62	3.591 (3)	171
C155—H15R···O42	0.98	2.56	3.531 (3)	169
C156—H15T···O41^{iv}	0.98	2.60	3.562 (3)	166

Symmetry codes: (i) $x, -y+\frac{1}{2}, z+\frac{1}{2}$; (ii) $x, -y+\frac{3}{2}, z-\frac{1}{2}$; (iii) $x, y-1, z$; (iv) $x, y+1, z$.

The X-ray intensities of (I*a*) were obtained with two different exposure times and rotation angles of 1° at 290 K. 364 φ and 455 ω scans were measured with an exposure time of 60 s per frame, and 364 φ scans with an exposure time of 12 s per frame. The X-ray intensities of (I*b*) were measured with a different crystal at 110 K and were obtained with two different data sets. For data set 1, 1383 φ scans and 1114 ω scans were measured with an exposure time of 10 s per frame and a rotation angle of 0.5° (overflow scans).

Table 2
Selected bond lengths (Å) for the molecules of (I*b*).

	X = 1	X = 2	X = 3	X = 4	X = 5	X = 6	$d_{max} - d_{min}$
Cr1—OX1	1.9572 (17)	1.9580 (17)	1.9690 (16)	1.9703 (16)	1.9651 (18)	1.9437 (17)	0.0266
Cr2—OX2	1.9541 (16)	1.9705 (17)	1.9662 (16)	1.9692 (16)	1.9569 (17)	1.9481 (16)	0.0224
Cr3—OX3	1.9614 (17)	1.9645 (18)	1.9676 (16)	1.9700 (17)	1.9564 (17)	1.9623 (16)	0.0136
Cr4—OX4	1.9640 (17)	1.9685 (18)	1.9696 (16)	1.9704 (17)	1.9663 (17)	1.9460 (16)	0.0244
Cr5—OX5	1.9602 (17)	1.9672 (17)	1.9673 (17)	1.9670 (17)	1.9561 (18)	1.9567 (17)	0.0166
Cr6—OX6	1.9566 (17)	1.9750 (17)	1.9682 (16)	1.9629 (17)	1.9501 (17)	1.9645 (16)	0.0249
Average	1.9589	1.9673	1.9680	1.9683	1.9585	1.9536	

Note: X = 1–6 for molecules 1–6.

Table 4
Averaged C—H···O interactions (Å) of ligands C1*X*–C5*X*, C5*X*–C10*X* and C11*X*–C15*X* for (I*b*).

D—H···*A*	H···*A*	*D*···*A*
C5*X*—H···O5*Y*	2.49	3.45 (2)
C10*X*—H···O1*Y*	2.57	3.55 (4)
C15*X*—H···O4*Y*	2.60	3.57 (2)

Notes: calculation of the average values used [($\sum$C*X*—H*XY*···O*X*)/6], with *X* = 1–6 for molecules 1–6. *Y* takes labels and symmetry codes from Table 3.

Table 5
Averaged C—H···O interactions (Å) for molecules 1–6 of (I*b*).

Group	Molecule	H···*A*	*D*···*A*
1	1	2.57	3.54 (7)
1	2	2.56	3.53 (9)
1	4	2.56	3.54 (9)
2	3	2.55	3.51 (4)
2	5	2.54	3.51 (4)
2	6	2.54	3.51 (5)

Note: calculation of the average values used [(C5*X*—H5*X*···O5*X* + C10*X*—H10*X*···O1*X* + C15*X*—H15*X*···O4*X*)/3], with *X* = 1–6 for molecules 1–6.

Table 6
Intensity statistics in (I*b*).

	Reflections	$\langle I \rangle$	$\langle \sigma \rangle$	$\langle I \rangle / \langle \sigma \rangle$	$\langle I/\sigma \rangle$
A	3115	23111.90	467.53	49.43	32.17
B	6216	1652.16	95.29	17.34	13.73
C	9320	138.88	59.67	2.33	2.31

Notes: *A*: $h = 2n$ and $l = 3m$ (*m* and *n* are integers); *B*: $h \neq 2n$ and $l \neq 3m$ (*m* and *n* are integers); *C*: neither *A* nor *B*.

The data were integrated with *EVAL14* (Duisenberg *et al.*, 2003). Only reflections with $I > 10\sigma(I)$ were used. For data set 2, the same experiment was repeated with an exposure time of 50 s per frame. *DENZO* and *SCALEPACK* (Otwinowski & Minor, 1997) were used for the integration of the intensities of all data. The two data sets were scaled and corrected for absorption with *SORTAV* (Blessing, 1987). All H atoms were introduced in geometrically idealized positions (C—H = 0.93–0.98 Å), refined with a riding model and subsequently confirmed in contoured difference Fourier maps. Their isotropic displacement parameters were constrained [U_{iso}(H) = 1.2U_{eq}(C) for H atoms of the central C—H groups and U_{iso}(H) = 1.5U_{eq}(C) for methyl H atoms].

For (I*a*), data collection: *COLLECT* (Nonius, 1999); cell refinement: *PEAKREF* (Schreurs, 2005); data reduction: *EVAL14* (Duisenberg *et al.*, 2003) and *SADABS* (Sheldrick, 2002); program(s) used to solve structure: coordinates taken from the isostructural α-Co(acac)$_3$ compound (von Chrzanowski *et al.*, 2007*b*). For (I*b*), data collection: *COLLECT* (Nonius, 1999); cell refinement: *HKL-2000* (Otwinowski & Minor, 1997); data reduction: *EVAL14* (set 1) (Duisenberg *et al.*, 2003), *HKL-2000* (set 2) and *SORTAV* (Blessing, 1987); program(s) used to solve structure: *SHELXS97* (Sheldrick, 1997). For both compounds, program(s) used to refine structure: *SHELXL97* (Sheldrick, 1997); molecular graphics: *PLATON* (Spek, 2003); software used to prepare material for publication: manual editing of *SHELXL97* output.

This work was supported by the Council for Chemical Sciences of the Netherlands Organization for Scientific Research (CW–NWO). We acknowledge A. V. Chuchuryukin for kindly providing the first sample of crystalline Cr(acac)$_3$.

Supplementary data for this paper are available from the IUCr electronic archives (Reference: BG3044). Services for accessing these data are described at the back of the journal.

References

Abrahams, S. C. & Keve, E. T. (1971). *Acta Cryst.* A**27**, 157–165.
Altomare, A., Burla, M. C., Camalli, M., Cascarano, G. L., Giacovazzo, C., Guagliardi, A., Moliterni, A. G. G., Polidori, G. & Spagna, R. (1999). *J. Appl. Cryst.* **32**, 115–119.
Astbury, W. T. & Morgan, G. T. (1926). *Proc. R. Soc. London Ser. A*, **112**, 448–467.
Beurskens, P. T., Admiraal, G., Beurskens, G., Bosman, W. P., Garćia-Granda, S., Gould, R. O., Smits, J. M. M. & Smykalla, C. (1999). *The DIRDIF99 Program System*. Technical Report of the Crystallography Laboratory, University of Nijmegen, The Netherlands.
Blessing, R. H. (1987). *Cryst. Rev.* **1**, 3–58.
Burla, M. C., Camalli, M., Carrozzini, B., Cascarano, G. L., Giacovazzo, C., Polidori, G. & Spagna, R. (2000). *Acta Cryst.* A**56**, 451–457.
Cascarano, G., Giacovazzo, C. & Luić, M. (1985). *Acta Cryst.* A**41**, 544–551.
Chrzanowski, L. S. von, Lutz, M. & Spek, A. L. (2006). *Acta Cryst.* E**62**, m3318–m3320.
Chrzanowski, L. S. von, Lutz, M. & Spek, A. L. (2007*a*). *Acta Cryst.* C**63**, m129–m134.
Chrzanowski, L. S. von, Lutz, M. & Spek, A. L. (2007*b*). *Acta Cryst.* C**63**, m283–m288.
Diaz-Acosta, I., Baker, J., Cordes, W. & Pulay, P. (2001). *J. Phys. Chem. A*, **105**, 238–244.
Duisenberg, A. J. M., Kroon-Batenburg, L. M. J. & Schreurs, A. M. M. (2003). *J. Appl. Cryst.* **36**, 220–229.
Geremia, S. & Demitri, N. (2005). *J. Chem. Educ.* **82**, 460–465.
Goldhaber, S. B. (2003). *Regul. Toxicol. Pharmacol.* **38**, 232–242.
Hon, P. K. & Pfluger, C. E. (1973). *J. Coord. Chem.* **3**, 67–76.
Hummel, W., Hauser, J. & Bürgi, H. B. (1990). *J. Mol. Graph.* **8**, 214–220.
Mackay, A. L. (1984). *Acta Cryst.* A**40**, 165–166.
Morosin, B. (1965). *Acta Cryst.* **19**, 131–137.
Naumov, V. N., Bespyatov, M. A., Basova, T. V., Stabnikov, P. A. & Igumenov, I. K. (2006). *Thermochim. Acta*, **443**, 137–140.
Nonius (1999). *COLLECT*. Nonius BV, Delft, The Netherlands.
Otwinowski, Z. & Minor, W. (1997). *Methods in Enzymology*, Vol. 276, *Macromolecular Crystallography*, Part A, edited by C. W. Carter Jr & R. M. Sweet, pp. 307–326. New York: Academic Press.
Pilati, T. & Forni, A. (1998). *J. Appl. Cryst.* **31**, 503–504.
Sabolović, J., Željko, M., Koštrun, S. & Janeković, A. (2004). *Inorg. Chem.* **43**, 8479–8489.
Schomaker, V. & Trueblood, K. N. (1998). *Acta Cryst.* B**54**, 507–514.
Schreurs, A. M. M. (2005). *PEAKREF*. Utrecht University, The Netherlands.
Sheldrick, G. M. (1997). *SHELXS97* and *SHELXL97*. University of Göttingen, Germany.
Sheldrick, G. M. (2002). *SADABS*. University of Göttingen, Germany.
Spek, A. L. (2003). *J. Appl. Cryst.* **36**, 7–13.
Wiberg, N. (1985). *Hollemann-Wiberg Lehrbuch der Anorganischen Chemie*, 91–100 Auflage, pp. 979–983. Berlin: Walter de Gruyter.